80655

ALPHA AND GAMMA RADIATION EFFECTS ON AIR-WATER SYSTEMS AT HIGH GAS/LIQUID RATIOS*

by

D.J . Wronkiewicz and J. K. Bates
Argonne National Laboratory
9700 South Cass Ave
Argonne, Illinois   60439
USA
Telephone (708)   252-4390

RECEIVED

MAR 0 1 1999

OSTI

MASTER

August 1993

DISCLAIMER

DISCLAIMER

Portions of this document may be illegible in electronic image products. Images are produced from the best available original document.

ALPHA AND GAMMA RADIATION EFFECTS ON AIR-WATER SYSTEMS AT HIGH GAS/LIQUID RATIOS

D. J. Wronkiewicz and J. K. Bates
Argonne National Laboratory

ABSTRACT

Radiolysis tests were conducted on air-water systems to examine the effects of radiation on liquid phase chemistry under high gas/liquid volume (G/L) ratios that are characteristic of an unsaturated nuclear waste repository setting. Test parameters included temperatures of 25, 90, and 200°C; gamma vs. alpha radiation; dose rates of ~3500 and 50,000 rad/h; and G/L ratios of 10 and 100.

Formate, oxalate, and total organic carbon contents increased during irradiation of the air-water systems in gamma and alpha tests at low-dose rate (~3500 rad/h). Increases in organic components were not observed for tests run at 200°C or high-dose rates (50,000 rad/h). In the tests where increases in organics occurred, the formate and oxalate were preferentially enriched in solutions that were rinsed from the test vessel walls.

Nitrate (NO_3^-) is the dominant anion produced during the radiolysis reactions. Significant nitrite (NO_2^-) also occurs in some high-dose rate tests, with the reduced form of nitrogen possibly resulting from reactions with the test vessels. These results indicate that nitrogen acids are being produced and concentrated in the limited quantities of solution present in the tests. Nitrate + nitrite production varied inversely with temperature, with the lowest quantities being detected for the higher temperature tests. The $G(NO_3^- + NO_2^-)$ values for the 25, 90, and 200°C experiments with gamma radiation are 3.2 ± 0.7, 1.3 ± 1.0, and 0.4 ± 0.3, respectively. Thus, the elevated temperatures expected early in the life of a repository may counteract pH decreases resulting from nitrogen acid production. Little variation was observed in G values as a function of dose rate or gas/liquid ratio.

The apparent $G(NO_3^- + NO_2^-)$ value for alpha exposure at 25°C is 2.4 ± 1.1, slightly lower than that for gamma exposure at the same temperature. The lower yields may result from partial attenuation of alpha particles in the thin films of water that condensed on the [241]Am foils used in the experiments. The alpha particle radiation being emitted from the waste after storage periods in excess of 300 years might still be of a sufficient intensity to acidify the thin films of water condensed on the waste. The

formation of nitrogen and carboxylic acids in air-water systems exposed to radiation from relatively long-lived alpha-emitting transuranic elements suggests that radiolytic product formation will be a long-term concern for repository performance.

1. INTRODUCTION

The emplacement of nuclear waste in a geologic repository will subject the immediate environment of the waste container to radiation effects. The waste container, and the radioactive waste itself in the event of container failure, will be exposed to radiolytic products formed by the interaction of radiation with the air and liquid present in the repository environment. The influence of these radiolytic products is an important consideration for radionuclide immobilization because of their ability to corrode the waste containers and radioactive waste forms, thereby increasing the potential for radionuclide release to the accessible environment.

The intensities of the various types of radioactivity emanating from glass and spent nuclear fuel waste forms will vary as the waste ages. During the first several hundred years of repository operation, the radioactive energy is expected to be dominated by beta and gamma emissions from fission products with relatively short half-lives, such as ^{137}Cs and ^{90}Sr (1). Transuranic elements that decay to emit alpha particles generally have longer half-lives (from hundreds to tens of thousands of years) and will become the dominant radiation source at longer times. Because of their low penetrability in solids, alpha and beta particles can interact with the environment surrounding the waste container only after it has been breached and the air/water environment of the repository has directly contacted the waste. Gamma radiation can penetrate the waste container walls and thus may interact with the environment surrounding the waste package immediately after emplacement. The relatively short half-lives of gamma-emitting sources, however, lessen their importance as the waste ages (1).

Many studies have been conducted to investigate the effects of radiation on glass alteration in air-water systems. Ionizing radiation will electronically excite and ionize water molecules and dissolved gases to form reactive radicals and new molecules (2). The predominant water radiolysis species include hydrated electrons (e^-_{aq}), hydrogen ions (H^+), hydroxyl ($\cdot OH$), hydroperoxyl ($HO_2\cdot$), hydrogen atoms ($H\cdot$), molecular oxygen anions (O_2^-), the molecular species hydrogen (H_2), and hydrogen peroxide (H_2O_2). Jones (3) has reported that irradiation of moist air produces nitric acid (HNO_3), nitrous oxide (N_2O), and ozone (O_3). Molecular nitrogen and carbon dioxide dissolved in the water may also undergo radiolytic decomposition, during which a several

step recombination of the dissociation products with oxygen, water, and other associated radiolytic products forms nitrogen and carboxylic acids (2, 4-6).

The efficiency of radiation in producing radicals or molecules is expressed as a *G value*, which is the average number of radiolytic species created (positive G) or destroyed (negative G) per 100 eV absorbed radiation energy. Because the solubility of nitrogen in water is low, G values for nitric acid production in air-saturated water are also small. The $G(NO_3^-)$ values reported for oxidized water systems irradiated by a variety of sources range from zero to less than 0.2 (7-12), while values for radiolytic production of nitric acid from moist air or air/liquid water systems are ~2.0 (3, 10, 12-15). The formation of nitric acid in the irradiated air and its subsequent condensation decreased the pH of deionized water (DIW) in these tests. The concentration of radiolytic acids within the small volumes of water present under high gas/liquid (G/L) ratios should rapidly lead to the formation of thin films of acidified water contacting the waste package components in a repository setting. Both nitric acid and water dissociation products have the potential to accelerate nuclear waste and metal container reaction rates (4, 15-18).

The overall purpose of this study is to examine the effects of radiation under high G/L ratios that are similar to those expected in an unsaturated repository setting. The tests are designed to examine the distributions and types of radiolytic products formed under a variety of test conditions. The temperatures and dose rates used in these tests were chosen to represent potential bounding conditions for the environment of the repository after waste emplacement. High-temperature and high-dose rate tests represent environmental conditions shortly after waste emplacement into the repository, while low-temperature and low-dose rate tests represent conditions expected several hundred years after waste emplacement. The inclusion of separate gamma and alpha tests also simulates an early repository scenario, dominated by beta and gamma radiation sources, and a long-term scenario dominated by alpha emissions from actinide sources. The G/L ratios used in these tests include those chosen to overlap with previously published results (G/L=10, 10) and those that simulate an unsaturated repository setting (G/L=100). Results from these tests will also form a basis for examining simulated waste reactions for glasses exposed to an irradiated atmosphere at high G/L ratios (19).

2. Experimental

2.1 Experimental Apparatus

Irradiation experiments have been performed using several configurations, with each test conducted in duplicate. A detailed experimental matrix appears in Table 1. All test environments simulated heterogeneous air-water systems, with enough high-purity DIW added to each vessel to saturate the air phase with water vapor and still retain a small amount of liquid water at the bottom of each vessel. Separate experiments were carried out under gamma and alpha irradiation to examine the effects of these two types of radiation on a high G/L ratio environment. A total of 48 gamma and 23 alpha radiolysis tests were performed. Additionally, eight tests were conducted without radiation exposure to provide element background concentrations.

2.1.1 Gamma Irradiation Tests

All gamma tests were performed in certified Parr reaction vessels made of Type 304L stainless steel (Parr Instrument Co., Moline, IL). These vessels have an internal volume of 21.4 cm^3. Tests were initiated by adding a premeasured amount of DIW to the bottom of each vessel, which was then fitted with an annealed copper gasket and hermetically sealed with a compression fitting.

Assembled vessels were irradiated by exposure to an external ^{60}Co gamma radiation source. Desired radiation dose rates were achieved by adjusting the distance between the ^{60}Co source and the test vessels. Dosimetry measurements were made by adding a ferrous sulfate solution to a glass tube, which was then inserted into a Parr vessel for irradiation. In this dosimetry technique, the absorbed dose is calculated from measurements of the amount of ferrous sulfate converted to ferric salt during irradiation (20). Measured dose rates were corrected for decay of the ^{60}Co source by applying the isochron equation (21) and a half-life of 5.272 years to derive the ^{60}Co decay constant. Median dose rates and cumulative doses absorbed by the solutions in the individual tests are given in Tables 1 and 2.

"Base-line" gamma tests were initiated by adding 0.22 mL of DIW into each 21.4 cm^3 stainless steel vessel to achieve a G/L ratio of ~100 (Table 1). These samples were exposed to a gamma dose rate of ~3600 rad/h at an ambient temperature of 25°C. These tests form a basis against which tests conducted under different conditions could be compared. For example, additional tests were run at variable temperatures (90 and 200°C) and dose rates (50,000 rad/h) to evaluate the effects of these parameters on

radiolytic product yields. Other tests were run to examine the effects of variable G/L ratios by adding 2.0 mL of DIW to achieve a G/L ratio of ~10 in the vessels. Test intervals for the various gamma experiments ranged from 7 to 180 days.

2.1.2 Alpha Irradiation Tests

The alpha tests utilized a ^{241}Am foil source (1500 μCi) coated with a thin gold film. Alpha energies for the ^{241}Am foil are ~4.6 MeV/alpha decay. In initial tests, the foil was cemented to a Lucite support rod, while in later experiments it was attached to a Type 304L stainless steel rod to eliminate potential sources of organic carbon contamination. This foil-rod assembly was attached to the underside of the vessel lid and inserted and sealed into a glass reaction vessel (Fig. 1). Measured internal volumes of the alpha test vessels were 1764 cm^3 with the rod assembly inserted. The assembled test vessel configuration ensured that all of the alpha particle energy was absorbed by the gas phase inside the vessel rather than the container walls.

Dosimetry measurements for the alpha-foil tests were performed at room temperatures using a N_2O gas dosimeter. This dosimeter determines the fraction of energy transferred to the gas phase by measuring the rate of N_2 gas production and comparing relative yields to an expected $G(N_2)$ value of 10.0. Nitrogen production was found to be linear for periods up to 24 days, with ~37% of the energy produced by the foils being deposited in the gas phase. The remainder of the alpha radiation energy was absorbed within the foil or by the protective outer film of gold. The calculated dose rate absorbed by the air surrounding the foil apparatus is ~2600 rad/h.

Alpha tests were initiated by adding ~17.6 mL of DIW into each 1764 cm^3 vessel to achieve a G/L ratio of ~100. The test conditions included exposure to alpha radiation at ambient temperatures of 25°C and periods of 14 to 129 days (Table 3). The similarity of experimental conditions between the alpha and base-line gamma experiments allows for a direct comparison between the effects of gamma and alpha irradiation in high G/L ratio environments.

2.2 Analytical Procedure

Upon completion of the prescribed test periods, the test vessels were removed from their respective radiation sources, and for the high-temperature tests, the vessels were cooled by immersing the vessel bottom in an ice bath. The weights of the test vessels were measured before and after testing to assess the extent of water loss. Water losses from the vessels of the 25 and 90°C gamma tests were insignificant, while average losses for the vessels of the 200°C gamma tests and 25°C alpha tests

represented ~15% of the total mass added to each test vessel. With the alpha tests, water loss increased as a function of increasing reaction time, however, a separate liquid-water phase remained in the bottom of all vessels during testing. The amount of retained water in the 200°C gamma tests were also always sufficient to maintain water vapor saturation inside the vessels. Loss of vessel pressure due to leakage may be expected to lower the concentration of "dry" atmospheric gases as the evaporation of water vapor continuously replaced gas components such as N_2, O_2, and CO_2. However, test results from vessels with large water losses indicate that vessel leakage has not influenced radiolytic product yields.

After weighing, the test vessels were opened, and "prerinse" aliquots were collected from the solution that accumulated in the vessel bottom. The prerinse solutions were analyzed for anions (NO_3^-, NO_2^-, Cl^-, SO_4^{2-}, F^-, $COOH^-$, and $C_2O_4^{2-}$) in the gamma and alpha tests as well as pH and carbon in the alpha tests. The surfaces of the test vessels and components were next sprayed with a fine mist of high-purity DIW to flush any radiolytic products that had condensed on the solid surfaces to the vessel bottom. Aliquots of this "rinse solution" were analyzed for anions, pH, and carbon for both the gamma and alpha tests. Corrections were applied to rinse solution analyses to account for elements that were with the prerinse aliquot. The rinse solution values reported in Tables 2 and 3 thus represent the total production (in micromoles) of elemental species in these tests. Actual concentrations of radiolytic products in the fluid condensed on the test vessel walls could not be determined because it was impossible to determine the actual weight distribution of water between the prerinse solution and the condensed fluid.

Anion concentrations were determined by ion chromatography, carbon with a Dohrman Total Carbon Analyzer, and pH with a combination electrode. All analytical measurements, including pH, were made at room temperature. Accuracy of anion analyses, reported as a percentage deviation from known values of a standard, range from 2 to 7%. Anion precision, determined by triplicate analyses of a single sample and reported as the coefficient of variation (standard deviation/mean x 100%), ranges from 2 to 5%. The accuracy determined for carbon values is within 3% error, while analytical drift over the time period required for pH analyses is ~0.02 pH units.

3. RESULTS

3.1 Gamma Irradiation Tests

3.1.1 Anion Concentrations

Significant amounts of nitrate (NO_3^-) and minor amounts of nitrite (NO_2^-) were produced during the gamma irradiation tests (Table 2). Between 40 and 80% of the nitrate and nitrite recovered from the vessels was concentrated in the prerinse solution, with the remaining fraction being located in the condensate that had collected on the vessel walls. The vessel bottom represents only 10% of the geometric surface area, indicating that nitrogen acids are preferentially concentrated in the prerinse solution at the vessel bottom. This concentration mechanism probably involves gravitational settling of aerosols and/or dripping of condensate from the walls into the bottom of the vessel. Concentrations of Cl^-, F^-, and SO_4^{2-} in irradiated solutions remained near background levels and, therefore, are not presented in the tables.

Data for G value yields are presented in Figures 2 and 3 for nitrate and nitrite summed together. This summation accounts for the influence of redox reactions on nitrogen acid yields. For most tests, the contribution of nitrite toward the total yields is negligible. An exception to this pattern is found in the high-dose gamma tests lasting 56 and 120 days, where nitrite represents ~1/10 of the total, and the gamma tests at G/L ratio = 10, where nitrite represent ~2/3 of the total yield.

The G values were calculated from the following equation:

$$G = (n \ N_A) \ / \ (D \ k \ gN_2 \ 100) \tag{1}$$

where n is the number of moles of NO_2^- + NO_3^- produced, N_A is Avogadro's number (6.022×10^{23} molecules mol^{-1}), D is the cumulative dose in rad, k is a constant 6.24×10^{13} eV g^{-1} rad^{-1}, and gN_2 is the number of grams of N_2 gas contained in a 21.4 cm^3 stainless steel vessel (10.48 g) for the gamma tests or 1764 cm^3 glass vessel (864.08 g) for the alpha tests. The additional value of 100 in the denominator reflects the G value representing the number of molecules produced per 100 eV.

Gamma tests run at ~50,000 rad/h and ~3600 rad/h do not show any variations in nitrate + nitrite G value yields, indicating no measurable effect on nitrogen acid formation as a function of dose rate (Fig. 2 and Table 2). Averaged G values were 3.2 ± 0.4 for the high-dose and 3.4 ± 0.9 for the low-dose rate tests at 25°C. However, the two samples exposed to the highest cumulative gamma doses (128 Mrad) displayed lower yields than that other tests. The validity of these latter results could not be determined because additional high dose samples were not run.

A comparison of 90°C tests run at G/L ratios of 10 and 100 also indicates no variation in average yields, although considerable data scatter occurs with both test conditions. The G values were 1.3 ± 1.0 for G/L = 100 and 1.6 ± 0.7 for G/L = 10.

Gamma tests run at 25, 90, and 200°C measure the formation of radiolytic products as a function of temperature. Results indicate that nitrate + nitrite production varies inversely with temperature, with the lowest quantities being detected for the higher temperature experiments (Table 2 and Fig. 3). Average $G(NO_3^- + NO_2^-)$ values for the rinse solutions are 3.2 ± 0.7, 1.3 ± 1.0, and 0.4 ± 0.3 for the 25, 90, and 200°C samples, respectively. The larger degree of data scatter for the tests at higher temperatures (Table 2) reflects analyzed concentrations that are approaching determination limits (~0.2 ppm). Pearson correlation coefficients are 0.95, 0.05, and 0.36 for the 25, 90, and 200°C tests, respectively. The results in Fig. 3 indicate that yields for the 90°C experiments are ~40%, while the 200°C yields are ~10% of those that characterize the 25°C tests. The 90°C yields are also similar to the $G(NO_3^-) = 1.9$ values obtained in neutron irradiation tests conducted at 80°C (10).

3.1.2 Solution pH

Solution pH measurements for the four G/L ratio = 10 tests indicate a pH decrease from the starting DIW solution to 5.9 ± 0.4. This value is indistinguishable from that expected for water in equilibrium with atmospheric CO_2 at ambient temperatures (pH = 5.7). Thus, radiation exposure had no discernible effect on the pH of these relatively dilute solutions.

The limited amounts of solution present in the G/L ratio = 100 tests precluded any direct measurement of solution pH. Nevertheless, solution pH values may be estimated based on the NO_3^- contents detected in the rinse. These calculations suggest that the limited quantities of solution will quickly attain a pH of ~3 after absorption of 5 Mrad and would continue to decrease to a pH of ~2 after 70 Mrad exposure (Fig. 4a). These calculations assume that nitric acid is the predominant acid present, complete dissociation of nitric acid occurs, and external pH buffering systems (e.g., bicarbonate) do not greatly influence the pH.

The previously discussed pH trends also represent the averaged pH for the entire 0.22 mL of solution initially present in the test vessels. This solution is actually divided into two fractions: a thin film of condensate located on the inside vessel walls and cap, and the solution remaining in the vessel bottom. The thin film of condensate may have a higher NO_3^- concentration than the solution at the vessel bottom because of the relatively larger surface area to liquid volume expected for the former. Thus, the

calculated pH values may be considered minimums if they are used to model the characteristics of solutions that condense on the surfaces of radioactive waste and waste containers.

3.1.3 Carbon Concentrations

Only the rinse solutions could be analyzed for carbon concentrations in the gamma tests, due to the small amount of fluid in each reaction vessel. Gamma radiation tests at low-dose rate show enriched concentrations of total carbon (TC), organic carbon (OC), and inorganic carbon (IC) relative to the background concentrations determined from blank test runs without radiation (Table 2). In contrast, carbon contents from the high-dose rate tests were at or below levels that characterized the background tests. Samples exposed to >35 Mrad cumulative exposure display the greatest depletion of carbon (Fig. 5a).

The carboxylic acids, formate and oxalate, occur at levels that parallel patterns shown by the OC data, suggesting that they are at least partially responsible for the observed increase in OC. The low-dose rate tests show production levels of formate and oxalate that are significantly enriched relative to blank tests without radiation (Table 2). Although there is a considerable amount of data scatter, the carboxylic acid contents appear to show a progressive increase with the absorbed dose. This increase is more strongly developed in the rinse solutions relative to the prerinse samples.

The various carbon fractions were also examined as a function of temperature. Overall results indicate that the OC fraction was lower in the 200°C tests relative to most of the 25 and 90°C tests; however, some overlap is noted between the two sample populations (Table 2 and Fig. 5b). No variation is noted in the IC concentrations as a function of temperature. Both the formate and oxalate contents show a progressive decrease with increasing temperature, especially in the prerinse fractions.

3.2 Alpha Irradiation Tests

3.2.1 Anion Concentrations

For the alpha tests, 30% of the total nitrate and nitrite was recovered from the prerinse solution that collected in the vessel bottom. This surface represents ~5% of the geometric surface area of the vessels. As with the gamma tests, this concentration of radiolytic products in the vessel bottom probably results from gravitational settling of aerosols and/or dripping of condensed solution from the vessel walls and foil assembly. Nitrate is the principal anion recovered in these tests, with minor amounts of nitrite also being present (Table 3). Tests run at 25°C with an alpha-radiation source

indicate a $G(NO_3^- + NO_2^-)$ value of 2.4 ± 1.1, with a calculated Pearson correlation coefficient of 0.89.

3.2.2 Solution pH

As with the gamma tests, the measured NO_3^- contents were employed to predict the solution pH. These calculations indicate a pH decrease to ~4 after 1 Mrad, and to ~2.5 after 7 Mrad exposure (Fig. 4b). The relatively large quantities of solution present in the alpha tests also allowed for a direct measurement of solution pH; however, the possible reactions between radiolytic acids and the glass test vessels may complicate interpretations of observed trends. Analytically measured pH values display a large degree of scatter and are notably higher than the calculated values (Fig. 4b). These comparisons suggest that the pH may have been buffered through reactions with the glass test vessels and/or dissolution of CO_2 from the vessel atmosphere.

3.2.3 Carbon Concentrations

Results from alpha tests with Lucite-supported ^{241}Am foils indicate that the Lucite has contributed to the OC production in the tests; therefore, no further consideration of these carbon values was given. With the stainless steel support rod tests, increases in average TC and OC values were observed relative to background tests without radiation, although the data do display a large amount of scatter (Table 3). These trends indicate that OC species are produced during alpha exposure. Both the rinse and prerinse solutions show a decrease in the IC with increasing exposure up to ~7 Mrad; thereafter an increase occurred. Contents of oxalate and formate in rinse solutions, as well as formate contents in prerinse solutions, display an increase after 5 Mrad of cumulative alpha exposure.

4.   DISCUSSION

Under the geologically unsaturated conditions expected at the proposed Yucca Mountain nuclear waste repository, the most likely mode of water contact is by condensation of small amounts of liquid water on the surfaces of waste containers or nuclear waste solids. In such a scenario, rapid concentration of radiolytic products may occur in the limited quantities of water present as thin films on the solid surfaces. In such a high G/L environment, any bicarbonate present in the thin films of water may be quickly overwhelmed by nitric acid produced in radiolysis reactions (15). Any nitric acid that subsequently condenses will acidify the solution and may accelerate the reaction rates of the containers or waste forms. The effectiveness of the bicarbonate buffer will

also be further reduced as radiolytic heating reduces the solubility of CO_2 in aqueous solutions.

The limited quantities of solution used in the gamma tests and the use of glass test vessels in the alpha tests do not allow for unambiguous interpretation of radiation effects on solution pH. However, measured pH values as low as 3.6 and the measured NO_3^- concentrations from the alpha radiation tests (Table 3 and Fig. 4b) do confirm that acids are being produced and concentrated in the limited quantities of solution present. These results are consistent with previously published observations noting the acidification of DIW in irradiated air-water systems at low G/L ratios (2, 3, 10, 12-14, 22).

Test results indicate that nitrate + nitrite production varies inversely with temperature, with the lowest quantities being detected for the higher temperature experiments (Fig. 3). This trend is important from the standpoint of waste form and container stability in that the highest radiation dose rates will occur early in the life of a nuclear waste repository, when waste package heating due to radioactive decay is also the greatest. Thus, the elevated temperatures expected early in the life of a repository may mitigate against large decreases in pH resulting from nitrogen acid production. Elevated repository temperatures should also hinder the formation of carboxylic acids due to the reduced solubility of CO_2 in heated waters.

The present 90°C gamma tests allow a comparison of the NO_3^- yields with the 80°C neutron-dominated irradiation tests of Linacre and Marsh, who reported $G(NO_3^-) = 1.9$ (10). The average yield, $G(NO_3^- + NO_2^-) = 1.3 \pm 1.0$, is reduced slightly relative to the Linacre and Marsh data, although the present data display a considerable amount of scatter. A decrease in G yields at 90°C, relative to the 80°C Linacre and Marsh results, is expected based on previously discussed temperature effects on nitrogen acid yields. Alpha yields of $G(NO_3^- + NO_2^- = 2.4 \pm 1.1$ from the present experiments are also similar to a $G(NO_3^-)$ yield of ~2.0 for alpha energy deposited in air above a ^{244}Cm-doped solution at 23°C (12).

The apparent alpha yields are slightly lower than the 3.2 ± 0.7 values determined for gamma radiation exposure at 25°C in this study. The decrease may be attributed to partial attenuation of the alpha particles in the thin film of water condensed on the ^{241}Am foils. If the energy transfer process (i.e., G values) were identical for both gamma and alpha radiation absorbed by the gas phase, then the observed decrease in alpha yields would represent an attenuation of approximately 25% of the alpha particle energy by the thin film of water. Additional tests will need to be performed in single-phase, moist-air systems to better constrain the nitrogen species G values for alpha radiation.

Burns et al. (2) indicate that complete attenuation of alpha particles should occur in a 40 μm film, while Garisto (23) indicates that >90% of the alpha particles will be attenuated within a 20 μm film of water. These values suggest an exponential change in the rate of alpha attenuation as a function of the thickness of the water film on the sample. Extrapolating these values to the observed decrease in alpha yields relative to gamma yields suggests that an average water film thickness of ~0.2 μm should result in the 25% attenuation of alpha energy deposited in the gas phase. In the actual test conditions, the thickness of the water layer varied from the top to the bottom of the foil under the influence of gravity and due to periodical dripping of water from the bottom of the foil. The relatively large degree of data scatter observed for the alpha tests may also reflect variable attenuation rates of alpha particles through films of water with uneven thicknesses.

Alternatively, the observed variation in nitrate + nitrite yields between the alpha and gamma tests may represent a fundamental difference in the mechanism of radiolytic product formation during ionization of moist air. Burns et al. (2) note that G values for liquid-water radiolysis species differ between systems that are irradiated by alpha vs. gamma radiation. It is conceivable, therefore, that G values for primary radiolytic species may differ for the two forms of radiation. These differences may arise due to variations in the efficiencies of different forms of radiation in breaking bonds in atmospheric gases.

The lack of variation in nitrogen acid yields, as a function of cumulative dose, between gamma radiolysis tests run at ~50,000 rad/h and ~3600 rad/h (Figure 2) result indicates that yields can be accurately modeled by considering the cumulative radiation dose over time. A comparison of different G/L ratio results suggests little variation in mean G yields, although a large degree of data scatter occurred under both test conditions (Table 2). The presence of large volumes of liquid water in air-water systems influences the radiolysis product concentrations by displacing equivalent volumes of the air phase where nitrogen acids are produced, diluting the radiolysis products that form, and offering a bicarbonate pH buffering reservoir for radiolysis reactions (2, 15, 19, 24).

Radiolysis of water may increase the redox potential (Eh) of the irradiated solution. During water irradiation, equal amounts of reducing and oxidizing species will be formed. The H_2 produced during radiolysis is chemically inert toward low-temperature (<100°C) aqueous reactions and has a high diffusional mobility relative to other radiolytic products (5, 25). The H_2 may thus be separated from the aqueous system, increasing the overall oxidation state of the irradiated fluid. With spent fuel

radiolysis, O_2^- and •OH are the predominant oxidizing agents, followed by H_2O_2, then O_2 (26).

An examination of the relative rates of NO_3^- versus NO_2^- production in the irradiated test solutions may offer some insight into the redox environment of the present tests. Nitrous acid (HNO_2) is thermally unstable and will decompose to nitrate according to the following reaction (27, 28):

$$3HNO_2 \rightarrow H^+ + NO_3^- + 2NO + H_2O \qquad (2)$$

The NO produced in this reaction would be rapidly oxidized in irradiated solutions to NO_2, which would then react with water to form equimolar amounts of NO_3^- and NO_2^- (28). The NO_2^- formed in this later step would then reprotonate to renew the cycle. Nitrous acid may also dissociate in the presence of radiolytically produced hydrogen peroxide to form nitrate according to the following reaction (27):

$$H_2O_2 + HNO_2 \rightarrow H^+ + NO_3^- + H_2O \qquad (3)$$

As a result of reactions in equations 2 and 3, all NO_2^- initially formed during radiolysis reactions will eventually be converted to NO_3^- (28).

A comparison of the nitrate and nitrite levels from the present set of tests indicates that nitrate is the predominant species formed under most test conditions, while nitrite concentrations are typically below levels of determination (Tables 2 and 3). Total recovered nitrite values are generally <0.05 micromoles for the 0.22 mL of solution in the gamma tests and <1.0 μmole for the ~18 mL of solution in the alpha tests. An interesting feature of the gamma tests is that the NO_3^-/NO_2^- ratios are lower in the rinse aliquots due to a slight increase in nitrite levels. Reactions between the thin films of condensed water and the stainless steel vessel walls may have caused this increase due to consumption of H_2O_2 that inhibits the progress of the reaction given by equation 3. Alternatively, ferrous iron released during corrosion of the vessels may reduce nitrate to nitrite (28). Minor surface pits were observed on a few of the vessels after the tests were completed.

The amount of nitrite produced increases substantially for gamma radiolysis tests exposed to more than 68 Mrad of cumulative radiation energy (Table 2). This change occurs when the increased acidification of the solutions due to nitric acid generation would be expected to destabilize nitrous acid (28). Oxygen depletion in the gas phase is probably not responsible for the observed NO_2^- increase because only 3%

of the oxygen present in the vessels is required to produce the nitrate in these tests. Furthermore, oxygen consumption may actually be lower if oxidizing contributions from water radiolysis products, such as O_2^-, $\bullet OH$, and H_2O_2 (25), contribute to nitric acid generation. As previously discussed, reduction of the test solutions with ferrous iron from the stainless steel vessels may have caused the NO_2^- increase, but it is not known why this increase would occur in the higher cumulative dose tests.

Overall patterns developed with respect to carbon contents of the test solutions are difficult to evaluate due to the large amount of data scatter. Averaged values for both OC and IC rinse solution fractions are noted to increase during the low-dose gamma tests at 25 and 90°C relative to the levels that characterized background tests without irradiation (Tables 2 and 3; Fig. 5b). The most likely source for the OC generation in these solutions is through the conversion of dissolved carbonic acid species into OC (4). The absence of a corresponding decrease in the IC fraction during OC formation suggests that dissolution of CO_2 from the gas phase or reactions with the test vessel walls have released additional IC to the solution. Analyses were not performed to examine for CO_2 depletion in the gas phase. Increases were also observed in the OC and IC contents of the rinse relative to the prerinse solutions for the alpha tests. It appears that the test vessel apparatus may have contributed to this increase because similar concentrations were also observed in the rinse solutions of the background tests (Table 3).

Formate and oxalate were noted in the rinse solution fractions during both alpha and gamma radiation exposure. These organic species account for ~50% of the OC observed in the 25°C alpha and 90°C gamma tests, but only 5% of the OC observed in the 25°C low-dose rate gamma tests. Increases were not observed in the OC fraction of the prerinse solutions from either the gamma or alpha tests. The formation of oxalate and formate is favored under low pH and/or oxygen-free conditions that prevent carboxyl radicals (CO_2^-) from transferring charge to oxygen, thus allowing sufficient time for carbonyl dimerization into oxalate or reaction with hydrogen ions to produce formate (4, 28). Favorable conditions may exist for the formation of formate and oxalate in the thin films of water contacting the vessel components in these tests. Although NO_3^- preferentially collected in the prerinse solution, the proportion of water that condensed on the vessel walls, top, and support rods (in the alpha tests only) may be of considerably less volume than that at the bottom. If this premise is true, then the concentration of nitric acid in this limited volume of fluid may be greater than that of the prerinse solution. Higher nitric acid concentrations, combined with less oxidizing conditions (as evidenced by the reduced NO_3^-/NO_2^- ratios) of the condensed fluid on the walls, would favor the formation of formate and oxalate.

Organic carbon production and the amounts of oxalate and formate are diminished in the gamma tests at 25°C, 50,000 rad/h and 200°C, 3500 rad/h relative to levels produced in the tests at 25°C, 3600 rad/h and 90°C, 2600 rad/h (Figs. 5a and b). The lower amounts of these species in the high-dose rate tests do not appear to reflect the cumulative dose because the yields of organic species differ notably where the cumulative doses for the high- and low-dose tests overlap. The reduced levels in the elevated temperature tests are probably associated with the decreased solubility of carboxyl radicals and/or carbonic acids in aqueous fluids.

5. CONCLUSIONS

Radiolysis tests conducted in air-water systems with high G/L ratios indicate that nitrate is the predominant radiolytic product, with high NO_3^-/NO_2^- ratios indicating that oxidizing conditions persisted during irradiation. An increase in nitrite levels is noted in the high cumulative dose and low G/L ratio tests. These later increases are believed to result from reactions between the test solutions and stainless steel vessel walls. These results indicate that nitrogen acids are being produced and concentrated in the limited quantities of solution present in the tests.

There was little change in $G(NO_3^- + NO_2^-)$ values as a function of dose rate or gas/liquid ratios, but nitrogen acid production did vary inversely with temperature. Respective $G(NO_3^- + NO_2^-)$ values for the 25, 90, and 200°C experiments are 3.2 ± 0.7, 1.3 ± 1.0, and 0.4 ± 0.3. This trend is important from the standpoint of waste form and container stability in that the elevated temperatures expected early in the life of the repository may prevent large decreases in pH resulting from nitrogen acid production.

The apparent $G(NO_3^- + NO_2^-)$ values of 2.4 ± 1.1 for the alpha tests are slightly lower than the 3.2 ± 0.7 values determined for gamma tests at 25°C. The lower yields may results from partial attenuation of alpha particles in the thin film of water condensed on the ^{241}Am foils. The formation of nitrate and nitrite in alpha tests at a high G/L ratio indicates that nitrogen acids may still play a role in influencing nuclear waste form reactions under long-term (>300 years) unsaturated storage conditions, when alpha radiation from long-lived transuranic elements dominates emissions from the nuclear waste forms. Thus, the alpha radiation being emitted from the waste after 300 years may still acidify thin films of water that contact the waste. The acidification of these solutions will ultimately depend on the ability of the bicarbonate buffering reservoir to regenerate itself and neutralize the acids that form.

For tests run at temperatures of 90°C or less and dose rates of ~3500 rad/h, the contents of formate, oxalate, and total organic carbon increased as a consequence of radiation exposure. These organic fractions were preferentially concentrated in thin films of water that had condensed on the walls of the test vessels. The formation of oxalate and formate is favored under relatively low pH conditions that may be present in these thin films. These organics may influence the retentive properties of nuclear waste by complexing with and transporting radionuclides. No enrichment of organic components occurred when test vessels were irradiated at 200°C or at dose rates of ~50,000 rad/h.

6 .   ACKNOWLEDGMENTS

REFERENCES

1. W. J. Weber, "The Effect of Radiation on Nuclear Waste Forms," J. Min. Metals and Mat. Soc., pp. 35-39 (July 1991).

2. W. G. Burns, A. E. Hughes, J. A. C. Marples, R. S. Nelson, and A. M. Stoneham, "Effects of Radiation on the Leach Rates of Vitrified Radioactive Waste," J. Nucl. Mater. 107, 245-270 (1982).

3. A. R. Jones, "Radiation-Induced Reactions in the N_2-O_2-H_2O System," Radiation Res. 10, 655-663 (1959).

4. A. Barkatt, A. Barkatt, and W. Sousanpour, "Gamma Radiolysis of Aqueous Media and Its Effects on the Leaching Processes of Nuclear Waste Disposal Materials," Nucl. Tech. 60, 218-227 (1983).

5. J. E. Mendel (compiler), "Radiation Effects," in Final Report of the Defense High-Level Waste Leaching Mechanisms Program, Pacific Northwest Laboratory Report PNL-5157, pp. 5.0-5.18 (1984).

6. N. E. Bibler, "Leaching Fully Radioactive SRP Nuclear Waste Glass in Tuff Groundwater in Stainless Steel," Adv. in Ceram. 20, 619-626 (1986).

7. L. Dolle and J. Rozenberg, "Radiolytic Yields in Water Reactor System and Influence of Dissolved Hydrogen and Nitrogen," in Water Chemistry of Nuclear Reactor Systems, British Nuclear Society, London, p. 291 (1978).

8. D. Rai, R. G. Strickert, and J. L. Ryan, "Alpha Radiation Induced Production of HNO_3 During Dissolution of Pu Compounds," Inorg. Nucl. Lett. 16, 551-555 (1980).

9. H. K. Rae, G. M. Allison, A. R. Bancroft, W. Makintosh, J. F. Palmer, E. E. Winter, J. E. Lesurf, and S. R. Hatcher, "Experience with the Chemistry of Water in Moderator and Coolant Systems," Proc. Int. Conf. Peaceful Uses At. Energy, 3rd Ed., Vol. 9, p. 318, Geneva (1985).

10. J. K. Linacre and W. R. Marsh, The Radiation Chemistry of Heterogeneous and Homogenous Nitrogen and Water Systems, Chemistry Division, AERE Harwell Report AERE-R 10027 (1981).

11. W. J. Gray and G. L. McVay, Nitric Acid Formation During Gamma Irradiation of Air/Water Mixtures, Pacific Northwest Laboratories Report PNL-SA-12309 (1984).

12. D. T. Reed and D. L. Bowers, "Alpha Particle-Induced Formation of Nitrate in the Cm-Sulfate Aqueous System," Radiochim. Acta 51, 119-125 (1990).

13. W. Primak and L. H. Fuchs, "Nitrogen Fixation in a Nuclear Reactor," Nucleonics 13, 38-41 (1955).

14.   D. T. Reed and R. A. Van Konynenburg, "Effect of Ionizing Radiation on the Waste Package Environment," Am. Nucl. Soc. Proc., High Level Radioactive Waste Management Conf., Las Vegas, Nevada, pp. 1396-1403 (1991).

15.   D. J. Wronkiewicz, J. E. Young, and J. K. Bates, "Effects of Alpha and Gamma Radiation on Glass Reaction in an Unsaturated Environment," Mat. Res. Soc. Symp. Proc. 212, 99-106 (1991).

16.   G. L. McVay and C. Q. Buckwalter, "The Nature of Glass Leaching," Nucl. Tech. 51, 123-129 (1980).

17.   G. L. McVay, W. J. Weber, and L. R. Pederson, "Effects of Radiation on the Leaching Behavior of Nuclear Waste Forms," Nucl. Chem. Waste Mgmt. 2, 103-108 (1981).

18.   W. G. Burns, W. R. Marsh, and W. S. Walters, "The γ Irradiation-Enhanced Corrosion of Stainless and Mild Steels by Water in the Presence of Air, Argon, and Hydrogen," Radiat. Phys. Chem. 21, 259-279 (1983).

19.   D. J. Wronkiewicz and J. K. Bates, Reactions of Glass during Radiation Exposure at High Glass Surface Area/Liquid Volume (SA/V) Conditions, Argonne National Laboratory Report (in preparation).

20.   J. W. T. Spinks and R. J. Woods, An Introduction to Radiation Chemistry, John Wiley & Sons, New York, pp. 93-98 (1976).

21.   G. Faure, Principles of Isotope Geology, John Wiley & Sons, New York, pp. 66-67 (1986).

22.   S. L. Nicolosi, "A General Model for the Analysis of Groundwater Radiolysis," Mat. Res. Soc. Symp. Proc. 44, 631-640 (1985).

23.   F. Garisto, Ann. Nucl. Energy 16, 33 (1989).

24.   W. L. Ebert, J. K. Bates, T. J. Gerding, and R. A. Van Konynenburg, "The Effects of Gamma Radiation on Groundwater Chemistry and Glass Reaction in a Saturated Tuff Environment," Mat. Res. Soc. Symp. Proc. 84, 613-622 (1987).

25.   S. Sunder and D. W. Shoesmith, Chemistry of Uranium Dioxide Fuel Dissolution in Relation to the Disposal of Used Nuclear Fuel, Atomic Energy of Canada, Ltd., Report AECL-10395 (1991).

26.   D. W. Shoesmith, S. Sunder, L. H. Johnson, and M. G. Bailey, Mat. Res. Soc. Symp. Proc. 50, 309 (1985).

27.   W. L. Jolly, The Inorganic Chemistry of Nitrogen, W. A. Benjamin, New York (1964).

28.   R. A. Van Konynenburg, Radiation Chemical Effects in Experiments to Study the Reaction of Glass in an Environment of Gamma-Irradiated Air, Groundwater, and Tuff, Lawrence Livermore National Laboratory Report UCRL-53719 (1986).

Table 1. Sampling Matrix for Alpha and Gamma Irradiation Tests.

Test Type	Temperature (C)	~Dose Rate (rad/h)	Gas/Liquid Ratio	Test Length (Days)
Gamma -"Base Line"	25	3600	100	34, 56, 126
Gamma	25	50,000	100	7, 14, 28, 56, 120
Gamma	90	2600	100	49, 85, 122, 150, 171
Gamma	200	3500	100	49, 122, 156, 171, 180
Gamma	90	3500	10	56, 120
Alpha—Lucite Rod Support	25	2600	100	22, 31, 65
Alpha—Stainless Steel Support	25	2600	100	14, 33, 45, 60, 63, 110, 129

Table 2. Anion Results For Gamma Blank Tests (values in micromoles).

Test Type	Exps. Time (h)	Dose Rate rad/h	Cum. Exposure (Mrad)	NO3 Pre-Rinse	NO3 Rinse	NO2 Pre-Rinse	NO2 Rinse	Pre-Rinse NO3/NO2	Rinse NO3/NO2	Oxalate Pre-Rinse	Oxalate Rinse	Formate Pre-Rinse	Formate Rinse	TC	Rinse OC	IC
Gamma− Base Line	816	3600	3.02	0.06	0.22	< 0.01	0.02	>6.0	11	< 0.01	< 0.01	0.03	0.11	1.29	0.88	0.41
"	816	3600	3.02	0.10	0.27	0.01	0.05	10	5.4	0.03	0.02	0.26	0.41	2.28	1.50	0.78
"	1342	3600	4.97	0.04	0.33	< 0.01	0.01	>4.1	33	< 0.01	0.04	< 0.01	0.08	1.10	0.70	0.40
"	1342	3600	4.97	0.25	0.46	< 0.01	0.01	>25	46	< 0.01	0.03	< 0.01	0.07	0.53	0.22	0.31
"	3017	3600	10.86	0.37	0.71	< 0.01	0.02	>37	36	< 0.01	0.13	0.07	0.20	0.80	0.00	0.80
"	3017	3600	10.86	0.38	0.82	< 0.01	0.02	>38	41	< 0.01	0.01	0.08	0.26	1.91	1.06	0.85
"	3017	3600	10.86	0.22	0.56	< 0.01	0.02	>22	28	0.06	0.26	< 0.01	0.59	6.79	4.98	1.81
"	3017	3600	10.86	0.09	0.51	< 0.01	0.02	>9.0	26	0.06	0.06	0.10	0.20	2.05	1.22	0.83
Gamma−High Dose Rate	165	51,500	7.38	0.62	0.48	< 0.01	0.02	>62	24	< 0.01	< 0.01	nr	nr	0.35	0.24	0.11
"	165	51,500	7.38	0.56	0.47	< 0.01	0.02	>56	24	< 0.01	< 0.01	nr	nr	0.49	0.32	0.17
"	304	56,100	15.45	1.59	1.23	< 0.01	0.04	>159	31	0.01	0.03	< 0.01	0.13	0.65	0.40	0.25
"	304	56,100	15.45	1.44	1.21	< 0.01	0.04	>144	30	0.03	0.03	< 0.01	0.11	0.45	0.28	0.17
"	657	54,800	32.59	2.35	1.86	< 0.01	0.03	>235	62	< 0.01	< 0.01	< 0.01	< 0.01	0.32	0.13	0.19
"	657	53,200	31.67	2.16	2.05	< 0.01	0.04	>216	51	< 0.01	< 0.01	< 0.01	0.08	0.22	0.00	0.22
"	1324	51,500	61.42	4.94	4.22	0.54	0.26	9.2	16	< 0.01	< 0.01	< 0.01	< 0.01	0.11	0.03	0.08
"	1324	51,500	61.42	6.71	4.89	0.51	0.27	13	18	< 0.01	< 0.01	< 0.01	< 0.01	0.21	0.09	0.12
"	2805	51,400	128.46	6.34	5.06	0.48	0.24	13	21	< 0.01	< 0.01	nr	nr	0.29	0.19	0.10
"	2805	51,400	128.46	10.55	7.33	1.25	< 0.57	8.4	>13	< 0.01	< 0.01	nr	nr	0.31	0.23	0.08
Gamma 90 C	1179	2200	2.48	0.12	0.14	< 0.01	0.05	>12	2.8	< 0.01	0.04	0.06	0.10	1.37	0.80	0.57
"	1179	2200	2.48	0.04	0.05	0.02	0.03	2.1	1.7	0.04	0.04	0.07	0.06	0.48	0.25	0.23
"	2014	3400	6.24	0.01	0.03	< 0.01	0.06	>.52	0.50	0.02	0.02	< 0.01	< 0.01	0.26	0.09	0.17
"	2014	3400	6.24	0.01	0.03	0.01	0.05	0.61	0.60	0.04	0.04	< 0.01	< 0.01	0.14	0.00	0.14
"	2922	2200	6.14	0.15	0.18	0.05	0.07	3.0	2.6	< 0.01	0.02	< 0.01	0.47	0.63	0.33	0.30
"	2922	2200	6.14	0.05	0.08	0.06	0.08	0.83	1.0	< 0.01	0.02	0.07	0.63	2.20	1.43	0.77
"	4101	2200	8.61	0.33	0.32	< 0.01	0.04	>33	8.0	0.01	0.03	< 0.01	< 0.01	3.78	1.49	2.29
"	4101	2200	8.61	0.32	0.28	0.03	0.05	11	5.6	< 0.01	0.35	< 0.01	< 0.01	1.47	0.64	0.83
"	3470	3200	10.06	0.04	0.04	< 0.01	< 0.01	>3.5	>4.0	< 0.01	< 0.01	nr	nr	0.49	0.27	0.22
"	3470	3200	10.06	0.05	0.05	< 0.01	< 0.01	>4.7	>5.0	< 0.01	< 0.01	nr	nr	0.54	0.34	0.20

Table 2 (cont.) Anion Results For Gamma Blank Tests (values in micromoles)

Test Type	Exps. Time (h)	Dose Rate rad/h	Cum. Exposure (Mrad)	NO3 Pre-Rinse	NO3 Rinse	NO2 Pre-Rinse	NO2 Rinse	Pre-Rinse NO3/NO2	Rinse NO3/NO2	Oxalate Pre-Rinse	Oxalate Rinse	Formate Pre-Rinse	Formate Rinse	TC	OC	IC
Gamma 200 C	1179	4200	4.71	< 0.01	0.05	< 0.01	0.01	1.0	5.0	< 0.01	0.03	< 0.01	0.05	0.33	0.08	0.25
"	1179	4200	4.71	0.07	0.06	< 0.01	0.04	>7.0	1.5	< 0.01	0.03	< 0.01	0.07	0.38	0.04	0.34
"	3737	2400	8.22	0.02	0.02	< 0.01	< 0.01	>2.0	>2.0	< 0.01	< 0.02	nr	nr	0.10	0.05	0.05
"	4318	2400	9.50	< 0.01	< 0.01	< 0.01	0.02	1.0	<.50	< 0.01	0.01	nr	nr	0.11	0.07	0.04
"	4318	2500	9.93	< 0.01	0.01	< 0.01	0.03	1.0	0.33	< 0.01	0.01	nr	nr	0.09	0.06	0.03
"	3737	2200	7.47	< 0.01	< 0.01	< 0.01	0.03	1.0	0.33	< 0.01	< 0.01	nr	nr	0.06	0.06	0.00
"	2922	4200	11.98	0.05	0.12	< 0.01	0.02	>5.0	6.0	< 0.01	0.02	0.02	0.53	0.70	0.19	0.51
"	2922	4200	11.98	0.08	0.16	< 0.01	0.01	>8.0	16	< 0.01	0.02	0.02	0.39	0.98	0.24	0.74
"	4101	4200	16.83	0.02	0.12	< 0.01	0.01	>2.0	12	< 0.01	0.03	< 0.01	0.04	0.51	0.09	0.42
"	4101	4200	16.83	< 0.01	0.02	< 0.01	0.04	1.0	0.50	< 0.01	0.03	< 0.01	0.05	0.73	0.06	0.67
Gamma G/L=10, 90 C	1324	3200	3.84	0.04	0.04	0.06	0.09	0.54	0.44	0.01	< 0.02	< 0.01	< 0.01	0.27	0.27	0.00
"	1324	3200	3.84	0.06	0.08	0.07	0.12	0.83	0.67	< 0.01	< 0.02	< 0.01	< 0.02	0.32	0.27	0.05
"	2805	3700	9.26	0.04	0.05	0.16	0.19	0.23	0.26	0.01	< 0.02	nr	nr	0.27	0.27	0.00
"	2805	3700	9.26	0.01	0.03	0.07	0.13	0.15	0.23	< 0.01	< 0.02	nr	nr	0.32	0.27	0.05
Background 25 C	0	None	0.00	< 0.01	0.03	< 0.01	0.09	1.0	0.33	< 0.01	< 0.02	< 0.01	< 0.01	0.29	0.10	0.19
"	"	"	"	< 0.01	0.01	0.01	0.02	<1.0	0.50	< 0.01	< 0.01	nr	nr	0.50	0.50	0.00
Background 90 C	"	"	"	0.01	0.02	0.01	0.02	1.0	1.0	< 0.01	< 0.01	< 0.01	< 0.01	0.13	0.06	0.07
"	"	"	"	0.03	0.04	< 0.01	0.04	>3.0	1.0	< 0.01	< 0.01	nr	nr	0.44	0.44	0.00
Background 200 C	"	"	"	< 0.01	0.05	< 0.01	0.08	1.0	0.63	< 0.01	< 0.01	< 0.01	0.12	0.49	0.26	0.23
"	"	"	"	< 0.01	0.01	< 0.01	0.03	1.0	0.33	< 0.01	< 0.01	< 0.01	0.10	0.46	na	na

Rinse solutions represent total element recovery from test. The umole value for carbon is based on elemental carbon molecular weight of 12. TC, total carbon; OC, organic carbon; IC inorganic carbon; nr, spectrum peak not resolved. All tests at G/L = 100 unless otherwise noted.

Table 3. Anion Results For Alpha Blank Tests (values in micromoles).

| Test Type	Rx. Time (days)	Cum. Dose (Mrad)	NO3 Pre-Rinse	NO3 Rinse	NO2 Pre-Rinse	NO2 Rinse	PreRinse NO3/NO2	Rinse NO3/NO2	pH Pre-Rinse	Oxalate Pre-Rinse	Oxalate Rinse	Formate Pre-Rinse	Formate Rinse	Pre-Rinse TC	Pre-Rinse OC	Pre-Rinse IC	Rinse TC	Rinse OC	Rinse IC
Alpha-Lucite Rod	22	1.37	0.66	1.21	< 0.15	0.58	>4.3	2.1	7.05	< 0.20	< 0.35	1.11	2.11						
"	22	1.37	2.85	4.65	< 0.16	0.47	>18	9.9	6.90	< 0.20	< 0.38	< 0.24	< 0.44						
"	31	1.93	1.08	5.88	1.40	1.83	0.77	3.2	4.94	0.26	0.60	1.29	3.36						
"	31	1.93	2.36	7.88	0.17	< 0.21	14	>38	3.60	0.15	0.35	3.18	4.12						
"	65	4.06	3.66	15.7	< 0.38	< 0.79	>9.6	>20	3.83	< 0.99	< 2.06	< 0.78	< 1.61						
"	65	4.06	3.96	16.8	< 0.38	< 0.75	>10	>22	4.18	< 1.00	< 1.95	5.45	9.11						
Alpha-SS Rod	14	0.87	0.63	3.60	0.17	< 0.19	3.8	>19	6.94	< 0.19	< 0.35	0.49	1.50	10.83	1.86	8.97	24.69	8.78	15.91
"	14	0.87	1.12	0.93	0.65	1.80	1.7	0.52	7.20	< 0.19	< 1.54	0.59	2.38	15.28	4.78	10.50	52.26	28.48	23.78
"	33	2.06	1.93	7.37	< 0.35	< 0.67	>5.5	>11	6.98	< 1.29	< 2.44	0.43	1.87	7.70	0.18	7.52	22.02	6.75	15.27
"	33	2.06	1.47	7.90	< 0.31	< 0.60	>4.7	>13	6.82	< 1.13	< 2.20	0.41	2.89	10.52	0.00	10.52	35.68	15.57	20.11
"	46	2.87	3.44	24.0	0.10	0.27	35	89	4.60	< 0.12	< 0.33	1.76	3.83	8.18	6.24	1.94	30.36	22.69	7.67
"	46	2.87	2.84	26.4	0.16	0.54	17	49	5.61	< 0.12	0.72	< 0.07	< 0.18	5.18	3.01	2.18	16.21	9.90	6.31
"	60	3.74	4.11	15.3	< 0.28	< 0.58	>15	>26	6.55	< 1.01	< 2.13	< 0.57	< 1.19	15.68	6.66	9.02	35.98	18.89	17.09
"	60	3.74	3.72	15.8	< 0.31	< 0.59	>12	>27	6.80	< 1.15	< 2.17	< 0.64	< 1.21	6.75	0.29	6.46	24.90	10.30	14.60
"	63	3.93	1.29	2.06	< 0.07	< 0.14	>20	>15	4.10	< 0.12	0.37	1.41	2.47	8.10	6.92	0.00	14.00	10.14	3.86
"	63	3.93	1.21	13.1	< 0.06	< 0.13	>19	>101	4.74	< 0.11	0.32	1.38	2.19	5.68	3.76	1.92	8.74	4.72	4.02
"	110	6.86	3.77	33.4	< 0.03	< 0.10	>119	>334	4.07	< 0.06	0.80	1.28	2.62	6.24	4.14	2.10	17.39	12.55	4.84
"	110	6.86	3.37	37.3	< 0.02	< 0.12	>141	>311	5.10	< 0.04	0.75	2.32	4.17	6.60	5.70	0.89	19.19	18.28	0.91
"	129	8.05	22.4	41.6	< 0.27	< 1.03	>85	>40	7.41	< 0.97	< 3.79	nr	nr	37.29	12.80	24.49	62.43	25.07	37.36
"	129	8.05	6.31	39.5	nr	nr			5.63	nr	< nr	nr	nr	9.44	5.42	4.02	37.97	15.73	22.24
Background	46	None	< 0.07	1.24	< 0.09	0.29	0.74	4.3	6.69	< 0.11	< 0.30	< 0.06	< 0.17	3.18	1.87	1.32	23.27	15.72	7.55
"	110	None	0.11	0.74	0.23	< 0.33	0.49	>2.2	6.52	< 0.08	< 0.28	0.46	1.66	3.75	2.18	1.57	13.07	4.70	8.37

See Table 2 for explanation. All alpha radiation tests were run at 25 C, G/L ratio = 100, and gamma exposure of 2600 rad/h.

FIGURE CAPTIONS

Figure 1.   Experimental apparatus for alpha radiolysis tests.

Figure 2.   Total nitrate + nitrite in 25°C gamma tests as a function of cumulative
              dose. Two test configurations are compared with dose rates of 3600 and
              50,000 rad/h. The G = 3.2 line represents the average $G(NO_3^- + NO_2^-)$
              yield for all 25°C gamma tests. The Pearson correlation coefficient for
              the data is 0.95.

Figure 3.   Measured nitrate + nitrite formation in ~3500 rad/h gamma tests as a
              function of cumulative dose. Dotted lines represent average yields for
              tests at temperatures of 25, 90, and 200°C. Line for the 80°C trend
              derived from neutron irradiation study of Linacre and Marsh (10).
              Calculated Pearson correlation coefficients are 0.95, 0.05, and 0.36 for
              the 25, 90, and 200°C results, respectively.

Figure 4.   Solution pH plotted as a function of cumulative dose. Calculated pH values
              determined from NO_3^- solution concentration: (a) calculated pH values
              for gamma tests and (b) calculated and measured pH values for alpha
              tests.

Figure 5.   Measured organic carbon formation in gamma tests as a function of
              cumulative dose: (a) organic carbon contents for dose rates of 3600 and
              50,000 rad/h and (b) organic carbon for tests at temperatures of 25,
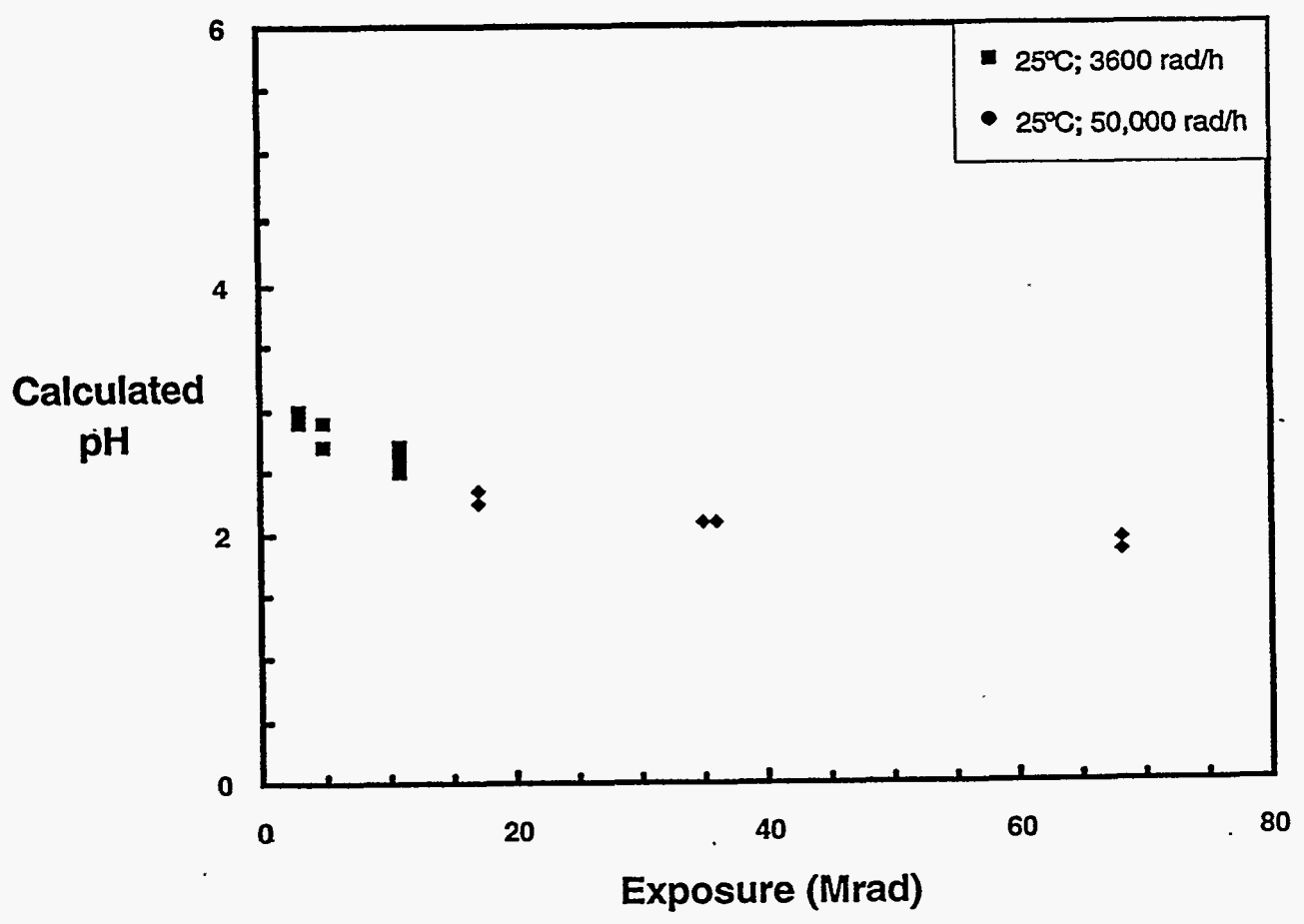   90, and 200°C.

Fig. 1

Fig. 2
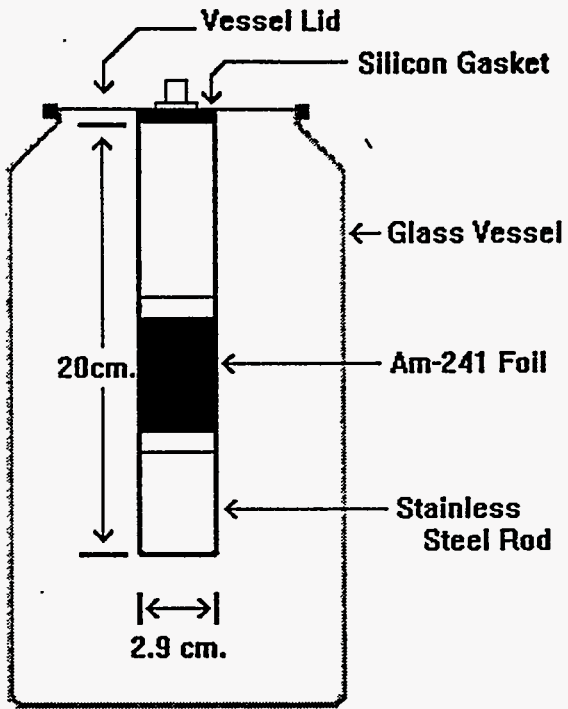
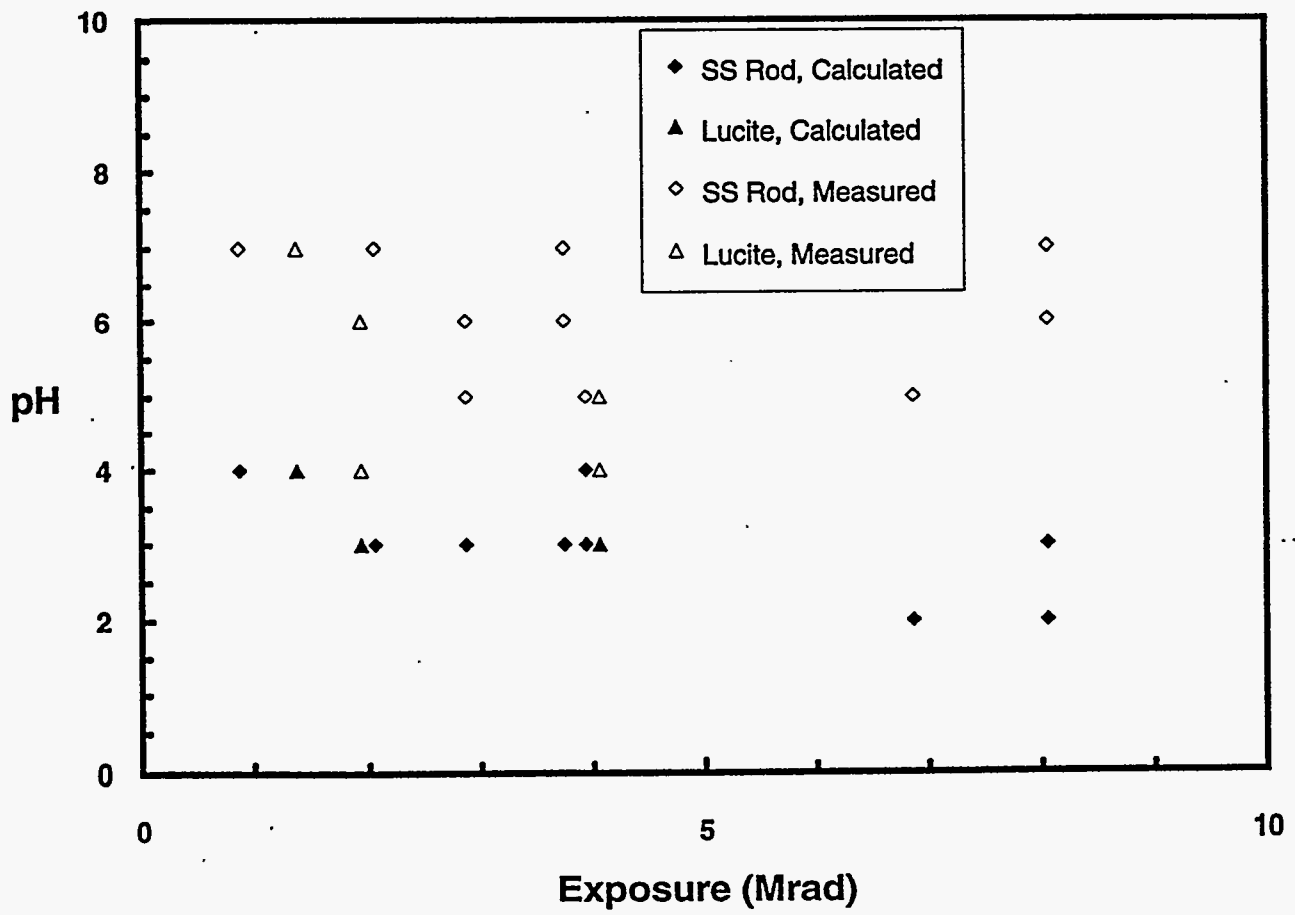**NOx Formation in Gamma Rinse Solutions**
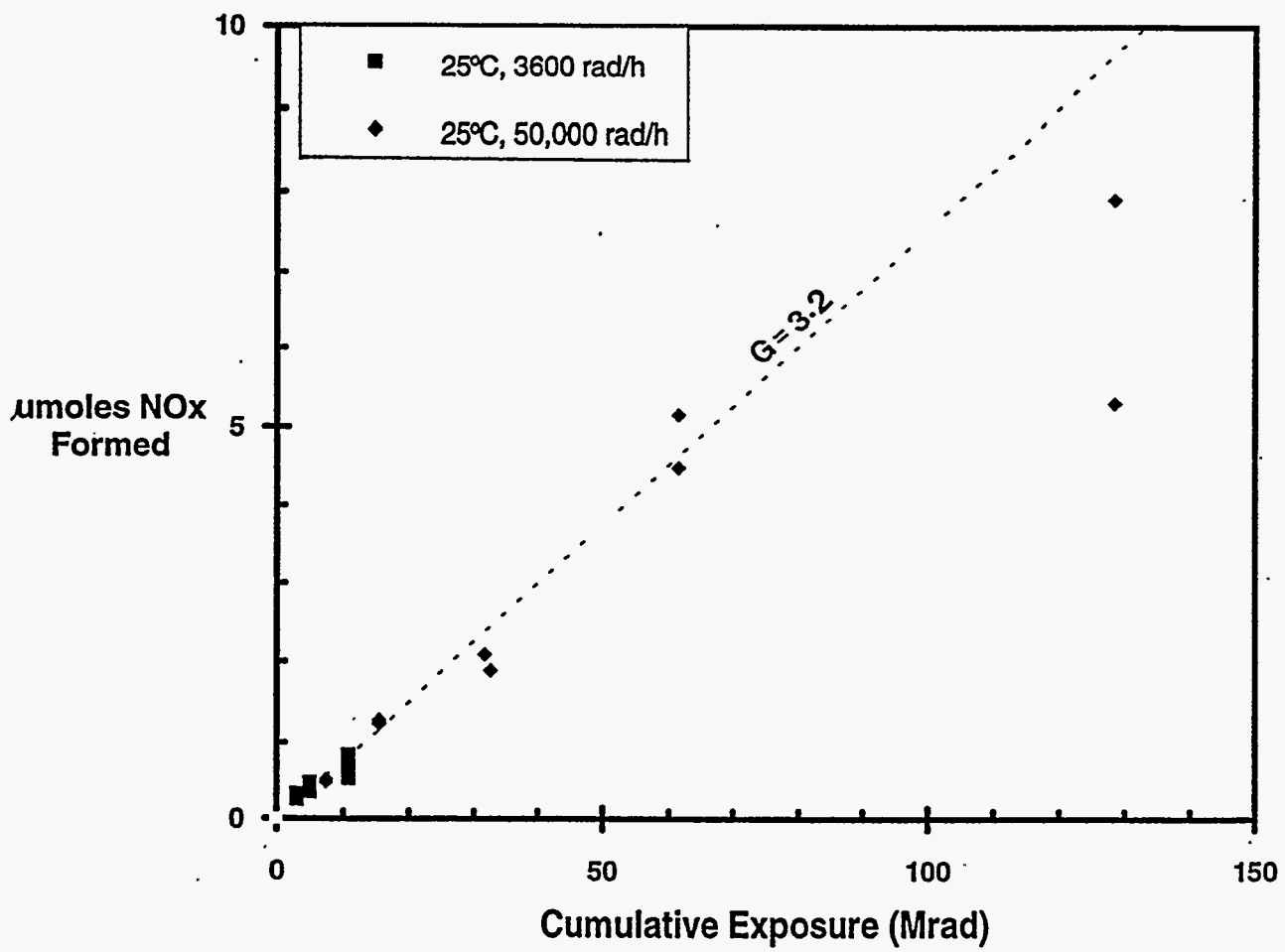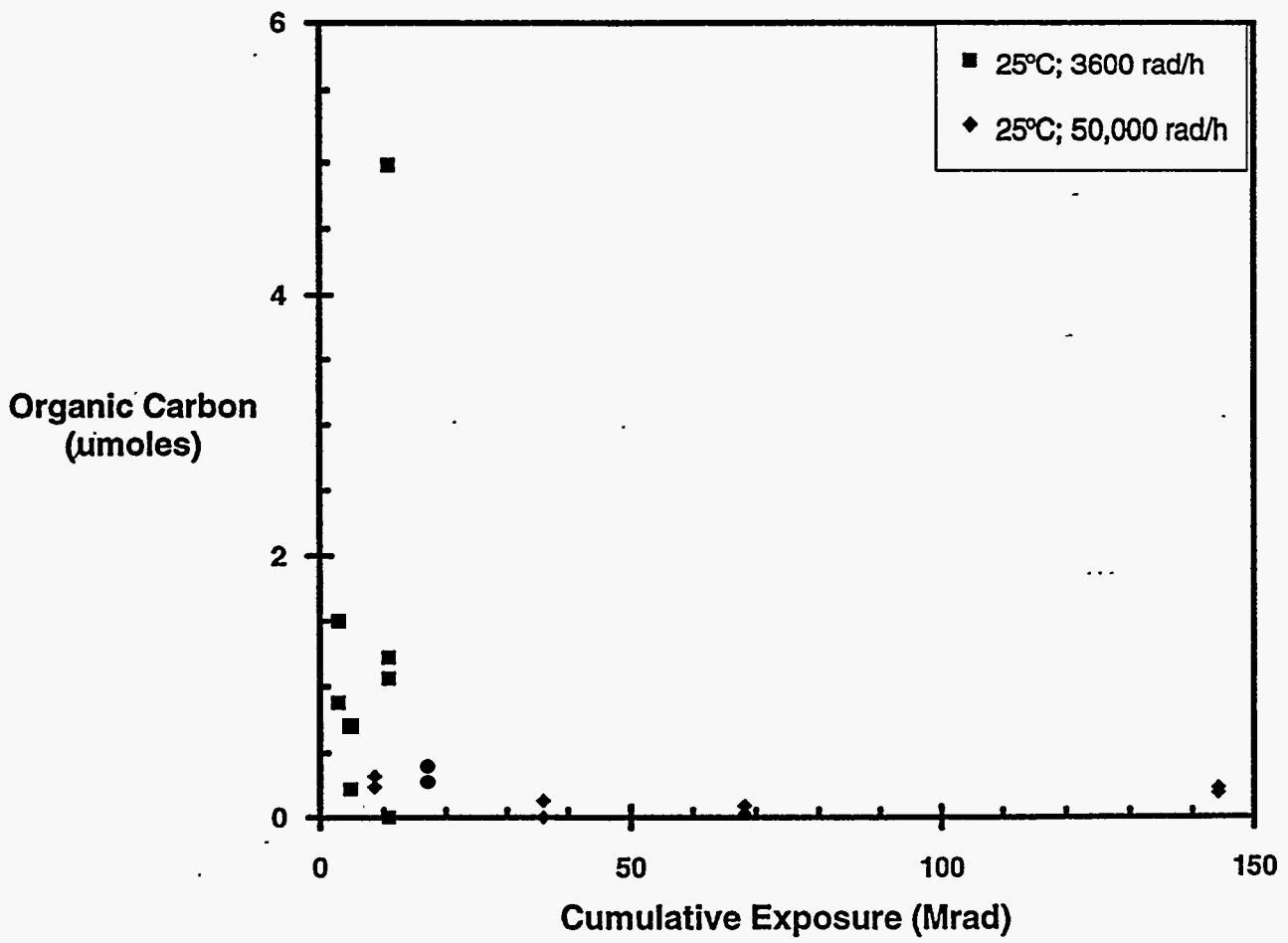
NOx Formation in Gamma Rinse Solutions
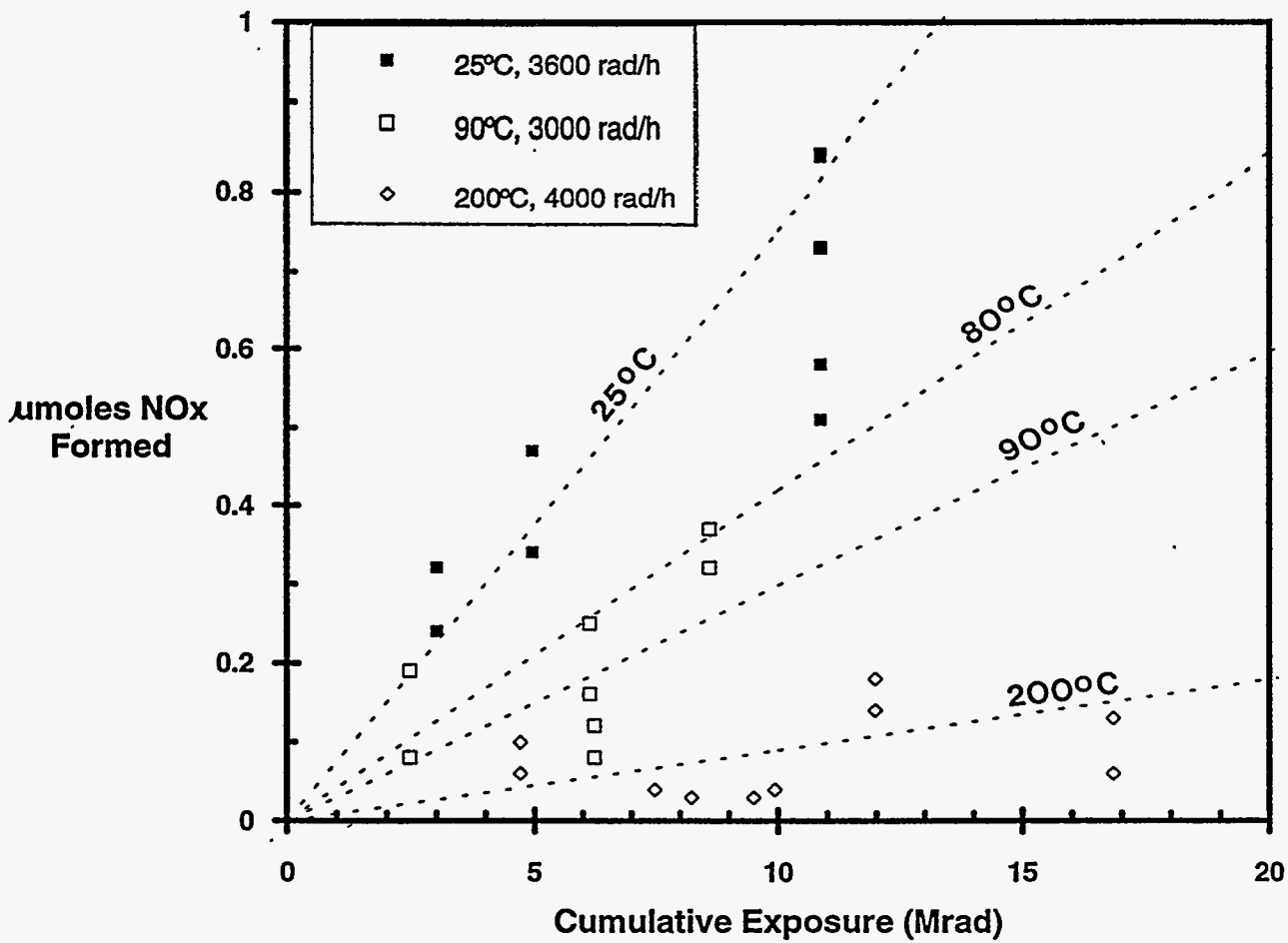
Calculated Gamma Rinse pH

Fig. 46

Alpha Rinse Solution pH vs. Exposure

Organic Carbon in Gamma Rinse Solutions

Organic Carbon in Gamma Rinse Solutions